



Research Article

ISSN : 0975-7384  
CODEN(USA) : JCPRC5

**Facile synthesis of ZnO-NiO nanocomposites for the removal of Hg(II) ions:  
Complete adsorption studies by using differential pulse anodic stripping  
voltammetry**

**K. Yogesh Kumar<sup>a</sup>, H. B. Muralidhara<sup>a\*</sup> and Y. Arthoba Nayaka<sup>b</sup>**

<sup>a</sup>Centre for Nanosciences, K.S. Institute of Technology, Visvesvaraya Technological University,  
Bangalore 560 062, India

<sup>b</sup>Department of PG Studies and Research in Chemistry, School of Chemical Sciences, Kuvempu  
University, Shankaraghatta 577 451, India

---

**ABSTRACT**

*In continuation to our recent study on the synthesis and characterization of metal oxide nanoparticles, in the present study the ZnO-NiO nanocomposites (ZNOs) has been evaluated for the removal of Hg(II) from the aqueous solution. The conditions for the sorption have been optimized. Kinetic and thermodynamic studies were performed to understand the adsorption behavior of the composite. The adsorption equilibrium data were modeled using the Langmuir and Freundlich isotherms, the data fitted more satisfactorily to Langmuir isotherms model when compare to Freundlich isotherm model. Based on Langmuir model,  $q_{max}$  was calculated to be  $1474.9 \text{ mgg}^{-1}$ . The adsorption showed pseudo second order kinetics indicating chemisorptions. The nanocomposites were successfully regenerated, regenerated ZNOs shows nearly one by third of the original adsorption capacity. The results indicate that the synthesized ZNOs could be employed as a low cost adsorbent for the removal of Hg(II) from aqueous solution.*

**Keywords:** Adsorption; DPASV; Mercury; Nanocomposites; Precipitation method.

---

**INTRODUCTION**

With the rapid development of modern industries, the environment has faced more and more contamination than in the past. It is well known that heavy metals present in water are extremely dangerous to environmental and human health [1]. Mercury is a heavy metal that is emitted to the atmosphere from natural processes such as volcanic and geothermal activity and via erosion from soils, vegetation and surface waters. However total inputs of Hg(II) to the atmosphere have increased in the past two centuries as a result of emissions of mercury from anthropogenic activities such as mercury mining, fossil fuel combustion and waste incineration [2].

The main toxicological effects of mercury include neurological damage, paralysis, blindness, and chromosomes breakage [3]. The heavy metals are stable and persistent environmental contaminants since they cannot be degraded and destroyed. In this context, the recovery of heavy metals from wastewater has become a major topic of research in water treatment [4].

A plethora of methods for heavy metal removal have been reported, e.g. chemical precipitation, membrane filtration, ion exchange, liquid extraction and electro-dialysis [5]. However, none of these methods has been widely used due

to the relatively high cost and low feasibility for small-scale industries. In contrast, the adsorption technique has become one of the most preferred methods for removal of heavy metals due to its high efficiency and low cost [6].

Among several materials used as adsorbents, activated carbons have been used for the removal of different types of emerging compounds in general but their use is sometimes restricted due to high cost [7]. This has resulted in attempts by various workers to prepare low cost alternative adsorbents which may replace activated carbons in pollution control through adsorption process and to overcome their economic disadvantages [8, 9].

Recently more attention was paid on mixed oxide nanoparticles as adsorbents due to its lower cost and higher adsorption capacity towards heavy metals [10]. The study of composite material i.e mixture consisting of at least two phases of different chemical compositions has been of great interest from both fundamental and practical point of view [11]. The physical properties of such materials can be combined to produce material of desired response. Composites have good potential for various industrial fields because of their excellent properties such as high hardness, high melting point, low density, low coefficient of thermal expansion, high thermal conductivity, good chemical stability and improved mechanical properties such as higher specific strength, better wear resistance and specific modulus [12].

The objective of this study is to investigate the possible use of the ZNOs as alternate adsorbents for the removal of Hg(II) from wastewater. The ZNOs are characterized by XRD, SEM and EDX. Batch experiments are carried out for the study on Hg(II) removal from aqueous solutions. The effects of pH, initial concentration, contact time and temperature on adsorption capacity of ZNOs is investigated. The Langmuir and Freundlich isotherm models are used to fit the experimental data. Pseudo-first-order and pseudo-second-order kinetic models are used to evaluate the kinetics of adsorption. Regeneration study is performed and adsorption mechanism is then discussed.

## EXPERIMENTAL SECTION

### Materials

All the reagents used in the experiments were of analytical grade and used as received without further purification. The stock solution ( $1000 \text{ mgL}^{-1}$ ) of Hg(II) was prepared by dissolving stoichiometric amount of corresponding mercuric chloride ( $\text{HgCl}_2$ ) in deionized water and further diluted to the desired concentrations for the experiments. Zinc nitrate ( $\text{Zn}(\text{NO}_3)_2 \cdot 6\text{H}_2\text{O}$ ), nickel nitrate ( $(\text{NiNO}_3)_2 \cdot 6\text{H}_2\text{O}$ ), triton X-100 ( $\text{C}_{14}\text{H}_{22}\text{O}(\text{C}_2\text{H}_4\text{O})_n$ ), sodium hydroxide (NaOH) were purchased from SD Fine chemicals, Mumbai, India.

### Instruments

The metal ion concentration was analyzed by DPASV using an electrochemical work station (CHI 660D). A three electrode system consisting of a glassy carbon ( $\text{Ø}=3\text{mm}$ ) as working electrode, saturated calomel as reference electrode and platinum wire as auxiliary electrode. X-ray diffraction (XRD) patterns were obtained on a Bruker D2 Phaser XRD system. Surface morphology (SEM) was studied using scanning electron microscope (JEOL JSM 840A), coupled with energy dispersive X-ray analyzer (EDX).

### Preparation of ZNOs

ZNOs were prepared through the co-precipitation method. In a typical synthetic procedure,  $\text{Zn}(\text{NO}_3)_2 \cdot 6\text{H}_2\text{O}$  and  $\text{Ni}(\text{NO}_3)_2 \cdot 6\text{H}_2\text{O}$  were used as the starting materials and NaOH as the precipitant. Both the metal salts ( $0.1 \text{ molL}^{-1}$ ) in a molar ratio of 1:1 were dissolved in 100 ml of deionized water, about  $50 \text{ mL}^{-1}$  triton X-100 was added as capping agent which inhibits the anomalous growth of metal hydroxide crystals during the course of precipitation. The NaOH was added drop wise to the vigorously stirred mixed solution. Then the resulting solution was kept at room temperature for about 3 hrs under constant stirring. The obtained slurry was centrifuged at 1000 rpm and precipitate was washed several times with water and alcohol, dried in an air oven for a period of 1-2 hrs at  $60^\circ\text{C}$ . Then powder is further heated in silica crucible for a period of 6 hrs at  $600^\circ\text{C}$ . Finally, the resulting adsorbent was stored in airtight container for further use to adsorption experiments.

### Adsorption experiments

To study the effect of parameters such as initial concentration, contact time, adsorbent dose, solution pH and temperature for the removal of Hg(II) on ZNOs were studied by batch adsorption techniques in a 250 ml of stoppered flasks (Erlenmeyer flasks) that contain definite volume (100 ml in each flask) of fixed initial concentration of adsorbates. The experiments were carried out in thermostated shaker at 200 rpm. The flasks were

then removed from the shaker and sample was withdrawn and analyzed by DPASV method, using electrochemical workstation. The amount of adsorbate adsorbed at equilibrium condition,  $q_e$  ( $\text{mgg}^{-1}$ ) was calculated by the following equation:

$$q_e = \frac{(C_0 - C_e)}{W} V \quad (1)$$

where  $C_0$  and  $C_e$  are the initial and equilibrium concentrations ( $\text{mgL}^{-1}$ ) respectively.  $V$  is the volume of solution (L) and  $W$  is the mass of adsorbent used (g).

Effect of pH on the adsorption capacity of metal ion was evaluated by agitating  $200 \text{ mgL}^{-1}$  metal ion solution with  $250 \text{ mgL}^{-1}$  of ZNOs for predetermined equilibrium time at pH ranging from 2.0 to 8.0. The pH of metal ion solution was adjusted by using 0.5 M HCl or 0.5 M NaOH. Similarly, the effect of adsorbent dosage (250, 500, 750,  $1000 \text{ mgL}^{-1}$ ) was also studied in batch experiments, while keeping metal ion concentration constant ( $200 \text{ mgL}^{-1}$ ). To evaluate the capacities of ZNOs to remove Hg(II), batch equilibrium experiments were performed with fixed adsorbent dosage of  $250 \text{ mgL}^{-1}$  at various initial concentrations ( $100\text{-}400 \text{ mgL}^{-1}$ ). The amount of metal ion adsorbed at equilibrium  $q_e$  ( $\text{mgg}^{-1}$ ) and the metal ion removal efficiency  $R(\%)$  were computed by Eq. (2) and (3) respectively.

$$q_t = \frac{(C_0 - C_t)}{W} \times V \quad (2)$$

$$R(\%) = \frac{(C_0 - C_t)}{C_0} \times 100 \quad (3)$$

## RESULTS AND DISCUSSION

### Characterization of adsorbent

Fig. 1 shows the XRD pattern of ZNOs. Some of the diffraction peaks like 31.7, 34.4, 36.2, 47.4 can be indexed to ZnO as per the JCPDS file 80-0075 but some other diffraction peaks like 43.2, 62.8, 75.1 are indexed to NiO as per the JCPDS file 78-0429. The dominance of ZnO over NiO is clearly seen. XRD also shows that ZNOs is a mixture of two phases: a ZnO-based wurtzite phase and a NiO-based cubic phase with the rock salt structure [13]. Furthermore the average crystallite size ( $D$  in nm) of ZNOs particles can be estimated according to the diffraction reflection by using Debye-Scherrer equation

$$D_P = \left( \frac{K\lambda}{\beta_{1/2} \cos \theta} \right) \quad (4)$$

where  $K$  is a constant equal to 0.89,  $\lambda$  is the X-ray wave length equal to  $1.54 \text{ \AA}$ ,  $\beta$  is the full width at half maximum and  $\theta$  is the half diffraction angle. The phase compositions of ZNOs calculated according to XRD quantitative analysis from profile-fitting peaks were listed in Table 1.

Fig. 2 shows the typical SEM micrographs of ZNOs under different magnification, it is clear from the SEM that single-phase primary particles, nearly of spherical shaped nanocrystallites were observed. Further it can be observed that each particle becomes distinguishable.

The chemical composition of ZNOs was investigated by EDX analysis. Fig. 3 depicts the typical EDX spectrum taken from ZNOs. The chemical analysis of the prepared nanocomposites measured by EDX analysis shows that only Zn, Ni and O signals have been detected, which indicated that the nanocomposites are indeed made up of Zn, Ni and O. No signal of secondary phase or impurity was detected, thus suggested the high purity of ZnO-NiO nanocomposites.

**Adsorption studies****Effect of initial concentration**

The effect of the initial Hg(II) concentration on the adsorption and adsorptivity (percentage of mercury adsorbed) is shown in Fig. 4. The adsorptivity decreases with increasing Hg(II) concentrations, whereas the adsorption capacity increases. Further it also indicates that sorbents active sites are saturated and further increase of the concentration will have no effect on the uptake. The maximal level of uptake adsorption reached for ZNOs was 83% with Hg(II) concentration of 100 mgL<sup>-1</sup>. In these conditions, the efficiency increases rapidly and over than 40% of the adsorbed Hg(II) occurred within 10 min using ZNOs. We noticed in the present study that 90 min was taken as adequate time for equilibrium.

**Effect of adsorbent dose**

Adsorbent dose is an important parameter in the determination of adsorption capacity. As the adsorbent dosage increases, the adsorbent sites available for Hg(II) metal ions are also increased and consequently better adsorption takes place. In the present study, the adsorbent dosages were varied from 250 to 1000 mgL<sup>-1</sup> in 200 mgL<sup>-1</sup> Hg(II) solutions, while all the other variables such as contact time, pH and temperature were kept constant. This method is also known as optimization based on one factor at a time where one parameter is varied, and the others are kept constant [14]. The results are shown in Fig. 5.

**Effect of pH**

The effect of pH on the surface species is responsible for the adsorption of the ions from the solution. The effect of pH on adsorption percentages of Hg(II) was investigated over the range of pH values from 2 to 8. As shown in Fig. 6 higher the pH, the higher is the sorption of the metal ions. At pH 2, the maximum amount sorbed is about 27% while by increasing the pH to 8, the adsorbed amount can reach 99%. As an explanation of sorption behavior, at high pH the surface charge of ZNOs is more negative due to presence of OH<sup>-</sup> groups that leads to formation of hydroxyl complexes. Formation of such hydroxyl compounds at higher pH is responsible for the uptake of the metal ions from the solution. In contrast, the low degree of sorption at low pH can be attributed to the competition of cations (mercury ions) and protons (H<sup>+</sup>) for the same sites, as well as the repulsion between ions of the same surface charge [15].

**Adsorption isotherms**

Analysis of isotherm data is important for predicting the adsorption capacity of the adsorbent, which is one of the main parameters required for the design of an adsorption system. Hg(II) sorption isotherms were fitted to both Langmuir and Freundlich equations. Fig. 7 and 8 shows the sorption isotherms for Hg(II) using ZNOs as sorbet. All the isotherm model parameters for the adsorption are listed in Table 2.

**Langmuir isotherm**

The Langmuir isotherm can be derived by assuming that only monolayer coverage of the adsorbent surface is possible. The non-linear equation of Langmuir isotherm model is expressed as follows:

$$q_e = \left( \frac{K_L C_e}{1 + a_L C_e} \right) \quad (5)$$

where  $q_e$  is the solid phase equilibrium concentration (mgg<sup>-1</sup>),  $C_e$  the liquid phase equilibrium concentration (mgg<sup>-1</sup>),  $K_L$  the Langmuir constant (Lg<sup>-1</sup>),  $a_L$  the Langmuir constant (Lmg<sup>-1</sup>), therefore a plot of  $C_e/q_e$  versus  $C_e$  (Fig. 7) gives a straight line of slope  $a_L/K_L$  and intercepts  $1/K_L$ . The theoretical maximum adsorption capacity ( $q_{max}$ ) corresponding to Langmuir constants is numerically equal to  $K_L/a_L$ . According to Langmuir model, adsorption was occurred uniformly on the active sites of the adsorbent. Once a sorbate occupied the site, no further adsorption could take place at this site. Thus experimental data were fitted to Langmuir adsorption isotherm model as shown in Table 2. The adsorption process of Hg(II) onto ZNOs could be considered the monolayer adsorption [16].

For predicting the favorability of an adsorption system, the Langmuir equation can also be expressed in terms of a dimensionless separation factor  $R_L$

$$R_L = \frac{1}{1 + a_L C_e} \quad (6)$$

where,  $R_L$  indicates the favorability and the capacity of the adsorbent/adsorbate system. When  $0 < R_L < 1$ , it represents good adsorption. The low values of  $R_L$  indicate that high and favorable adsorption and also indicated that the ZNOs is a suitable adsorbent for the adsorption of Hg(II) from aqueous solutions.

#### Freundlich isotherm

The Freundlich isotherm equation, the most important multilayer adsorption isotherm for heterogeneous surfaces is described by the following equation

$$q_e = K_f C_e^{1/n} \quad (7)$$

where  $K_f$  ( $\text{mgg}^{-1}$ ),  $1/n$  is the Freundlich adsorption constant and  $1/n$  is a measure of the adsorption intensity. The equation may be linearized by taking the logarithm on both sides:

$$\log q_e = \frac{1}{n} \log C_e + \log K_f \quad (8)$$

The linear plot between  $\log q_e$  versus  $\log C_e$  (Fig. 8) gives a straight line with  $K_f$  and  $1/n$  determined from the slope and intercept respectively. The magnitude of exponent  $n$  indicates the favorability of adsorbent/adsorbate system where values of  $n > 1$  represents favorable adsorption [17].

#### Adsorption kinetics

Sorption kinetics which is associated with solute uptake rate and determines the residence time of the adsorption reaction is an important property defining the sorption efficiency. Hence experiments were performed to have a clear insight into the kinetics of Hg(II) removal by the ZNOs. In order to reveal the adsorption mechanism, the kinetic data were fitted to Lagergren first-order, second-order and intraparticle diffusion model.

#### Pseudo-first-order kinetic model

The linear equation for pseudo-first-order equation is shown below:

$$\log(q_e - q_t) = \log q_e - \frac{k_1}{2.303} t \quad (9)$$

Where  $q_e$  and  $q_t$  are the amounts of adsorbate adsorbed ( $\text{mgg}^{-1}$ ) at equilibrium and at contact time  $t$  (min), respectively, and  $k_1$  is the pseudo-first-order rate constant ( $\text{min}^{-1}$ ). The first-order-rate constant  $k_1$  can be obtained from the slope of the plot  $\ln(q_e - q_t)$  versus  $t$  (Fig. 9). The  $R^2$  values obtained are relatively small and the experimental  $q_e$  values do not agree with the calculated values obtained from the linear plots. Which show that the model is not appropriate to describe the adsorption process.

#### Pseudo-second-order kinetic model

The pseudo-second-order equation based on equilibrium adsorption is expressed as follows [18]:

$$\frac{t}{q_t} = \frac{1}{k_2 q_e^2} + \frac{1}{q_e} t \quad (10)$$

where  $k_2$  is the rate constant of pseudo-second-order adsorption ( $\text{g} (\text{mg min})^{-1}$ ). The linear plot of  $t/q_t$  versus  $t$  is shown in Fig. 10 and the obtained  $R^2$  values are greater than 0.97 for the entire range of adsorption. It also shows a good agreement between the experimental and the calculated  $q_e$  values indicating the applicability of this model to describe the adsorption process of Hg(II) onto the ZNOs. Kinetic parameters for the adsorption of Hg (II) on ZNOs is shown in Table 3.

#### Intraparticle diffusion model

The probability of intra-particle diffusion was explored by using the intra-particle diffusion model.

$$Q_t = k_{id} t^{1/2} + C \quad (11)$$

where  $q_t$  is adsorption capacity at any time ( $t$ ),  $k_{id}$  is the intra-particle diffusion rate constant ( $\text{mg g}^{-1} \text{min}^{-1/2}$ ) and  $C$  ( $\text{mg g}^{-1}$ ) is a constant proportional to the thickness of the boundary layer. Plotting  $q_t$  versus  $t^{1/2}$  a “Weber-Morris plot” can give an indication of the dependency of adsorption on the intra-particle diffusion. If the plot gives a straight line, then the adsorption process is controlled by intra-particle diffusion only and if it exhibits multi-linear plots, then there are two or more steps affecting the adsorption process [19]. Fig. 11 shows the Weber-Morris plot of the Hg(II) adsorption on to ZNOs. It is clear from the graph that the adsorption of the Hg(II) on to ZNOs gives three different straight lines with good  $R^2$  (0.99). The first sharper portion was attributed to the diffusion of mercury through the solution to the external surface of adsorbent. The second portion described the gradual adsorption stage, where intraparticle diffusion was rate limiting. The third portion was attributed to the final equilibrium stage for which the intraparticle diffusion started to slow down due to the extremely low concentration left in the solution.

### Thermodynamic studies

The thermodynamic parameters such as enthalpy ( $\Delta H$ ), entropy ( $\Delta S$ ) and Gibbs free energy ( $\Delta G$ ) were examined in the range 303, 313 and 323K for the sorption systems of Hg(II) removal using the synthesized ZNOs, under optimized conditions mentioned earlier. Thermodynamic parameters were calculated by using the following equations:

$$k_c = \frac{C_a}{C_b} \quad (12)$$

$$\ln k_c = \frac{s^0}{R} - \frac{\Delta H^0}{RT} \quad (13)$$

where  $k_c$  is the distribution coefficient for the adsorption,  $\Delta H^0$  is the enthalpy change,  $\Delta S^0$  is the entropy change,  $\Delta G^0$  is the Gibb's free energy change,  $R$  is the gas constant,  $T$  is the absolute temperature,  $C_a$  is the Hg(II) adsorbed per unit mass of the adsorbent and  $C_b$  is the equilibrium adsorbate concentration in the aqueous phase. The values of  $\Delta H^0$  and  $\Delta S^0$  were determined from the slopes and intercept of the plot of  $\ln K_c$  versus  $1/T$  (Fig. 12).

While the Gibbs free energy change ( $\Delta G^0$ ) was calculated using the following equation:

$$\Delta G^0 = -RT \ln K_c \quad (14)$$

Table 4 illustrates the Gibbs free energy change ( $\Delta G^0$ ) for the studied range of solution temperature. It was noticed from this table that the value of  $\Delta H^0$  is positive, indicating adsorption of Hg(II) on to ZNOs is endothermic in nature. The positive value of  $\Delta S^0$  suggests that the process of adsorption is spontaneous and thermodynamically favorable. The positive entropy change also illustrates the increased randomness at the solid/solution interface. The negative values of  $\Delta G^0$  indicate the spontaneous nature of the process. The more negative values of free energy change with increase of temperature shows that, an increase in temperature favors the adsorption process of heavy metal ions on ZNOs nanoparticles.

### Regeneration studies

Regeneration of adsorbents is an important practice in environmental remediation. In regeneration tests ZNOs saturated with Hg(II) was added into 100 ml of 0.1M HCl solution. In a typical procedure; the solution was shaken on a rotary shaker at 200 rpm for 2 hrs at room temperature. The suspension was filtered and reused for the adsorption studies. For regeneration studies, experiments were carried out by taking  $250 \text{ mg L}^{-1}$  of adsorbent in  $200 \text{ mg L}^{-1}$  aqueous solution containing Hg(II) until equilibrium is reached. The removal percentage for first usage was found to be 80.36 and 53.17, 21.63 for first and second regenerations respectively (Fig. 13). As the number of regeneration increases, the poor efficiency of regenerated adsorbent in further adsorption studies is may be due to the strong interaction between the adsorbate and adsorbent, the number of active sites available on the surface of adsorbent decreases as the number of regeneration increases [20].

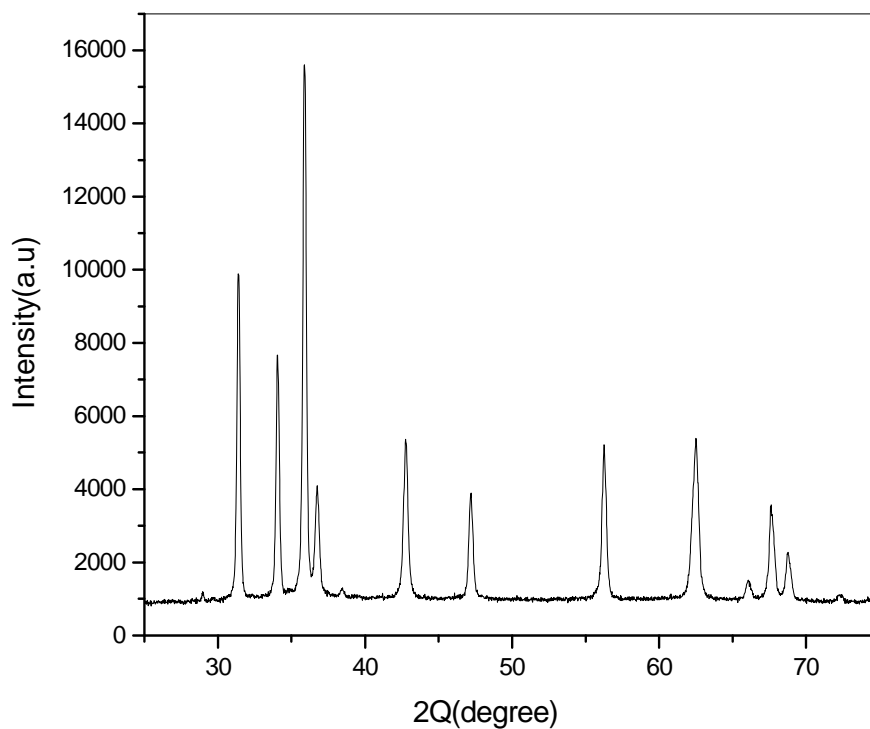


Fig. 1. Typical XRD pattern of ZnOs.

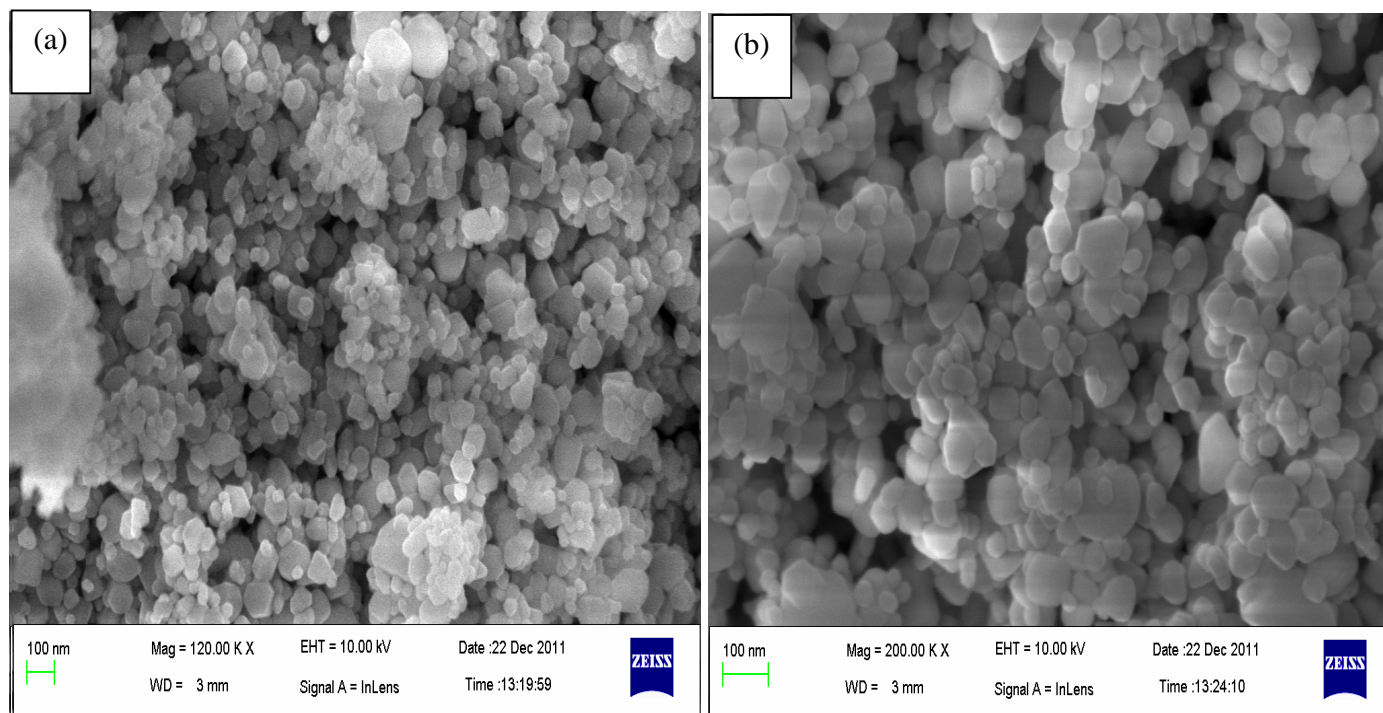


Fig. 2. Low (a) and High (b) magnification SEM micrographs of ZnOs.

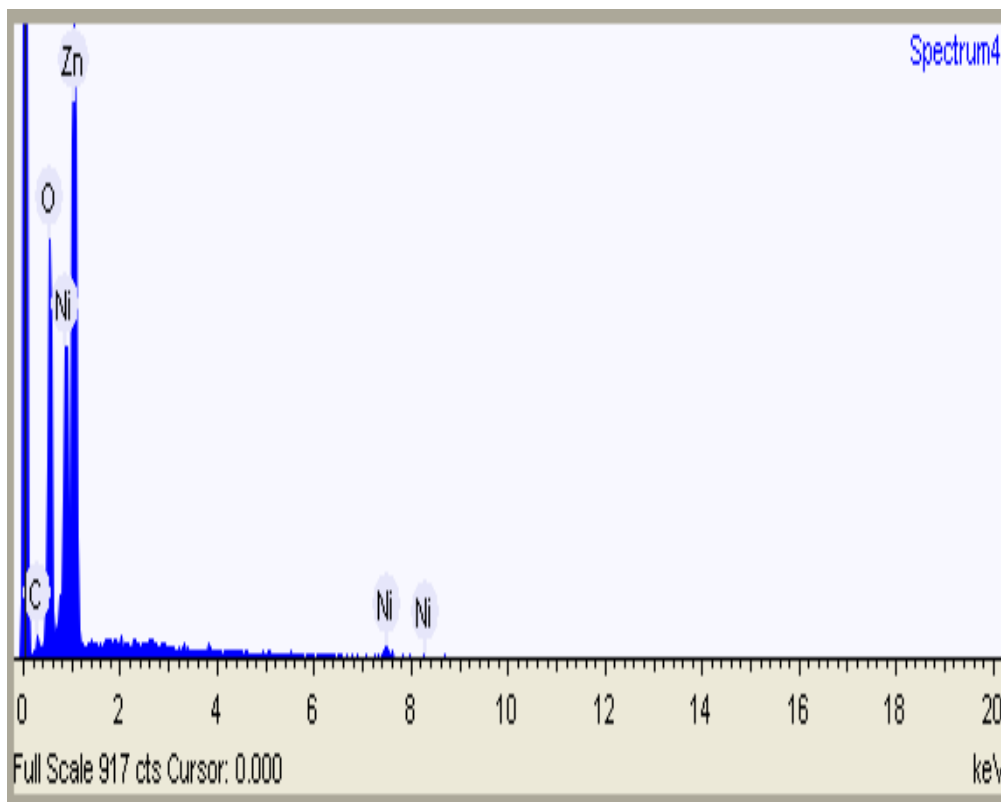


Fig. 3. EDX pattern of ZNOs.

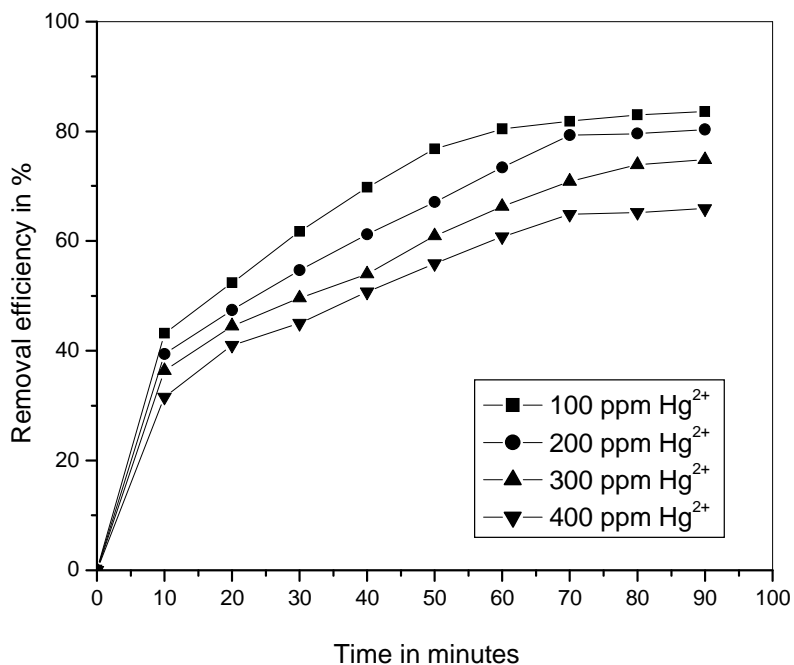


Fig. 4. Effect of contact time on adsorption of Hg(II) by ZNOs at different initial concentrations.

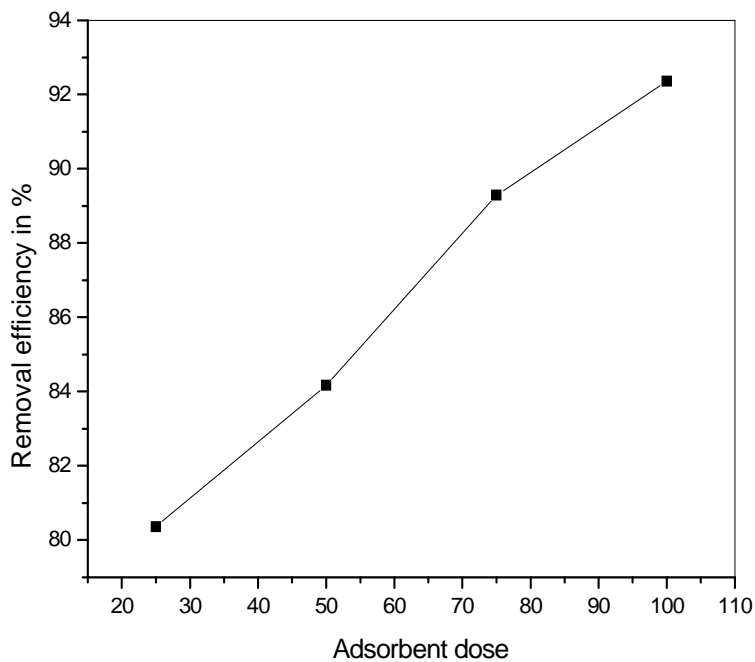


Fig. 5. Effect of adsorbent dosage on adsorption of Hg(II) by ZnOs.

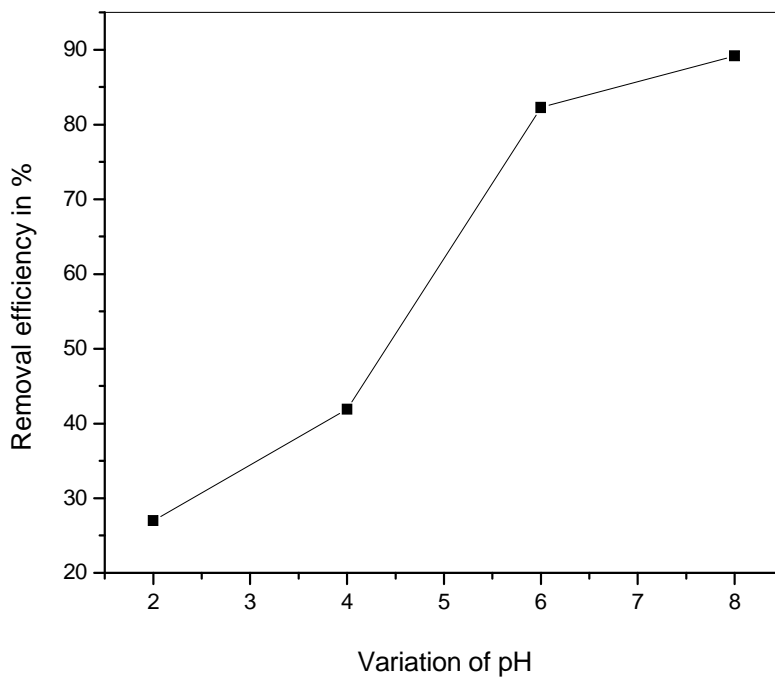


Fig. 6. Variation in removal efficiency of Pb(II) and Cd(II) on ZnOs as a function of pH.

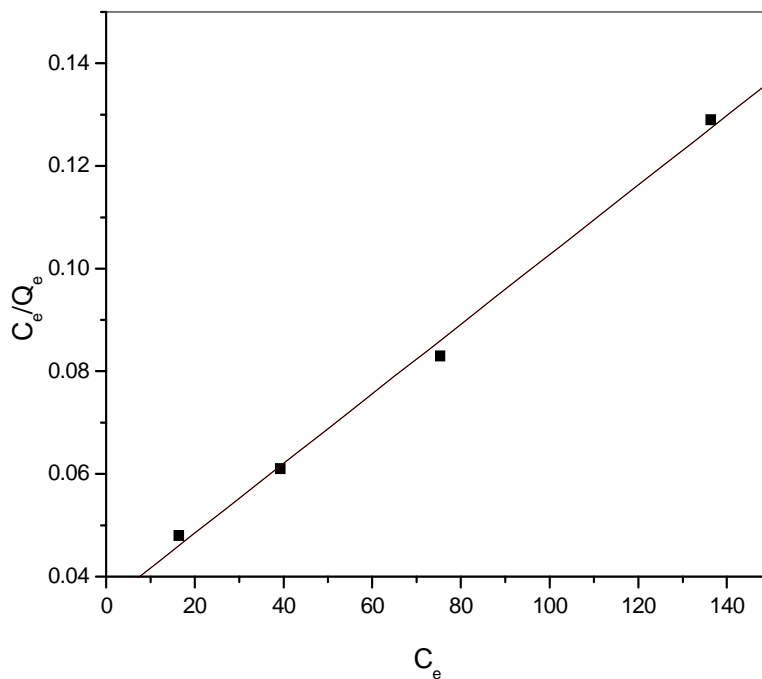


Fig. 7. Langmuir adsorption isotherm model for Hg(II) adsorption on ZNOs.

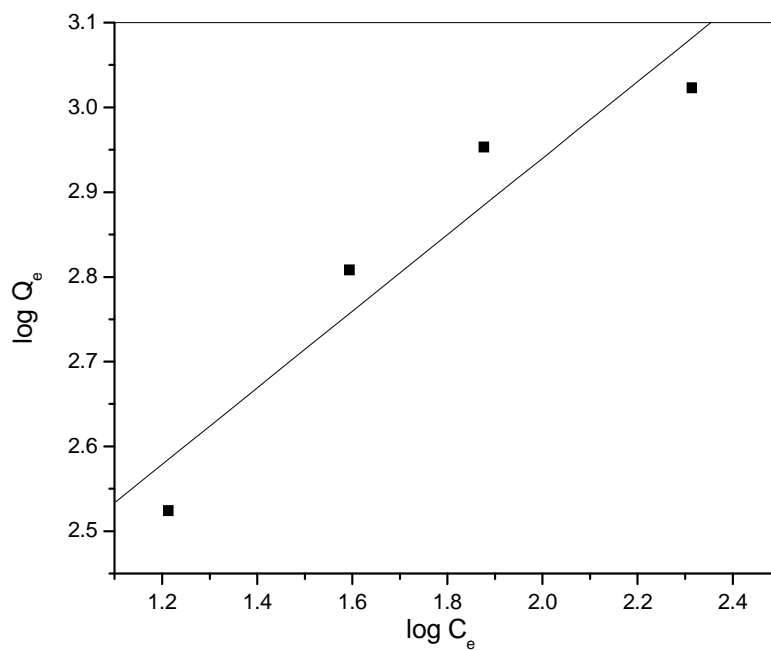


Fig. 8. Freundlich adsorption isotherm model for Hg(II) adsorption on ZNOs.

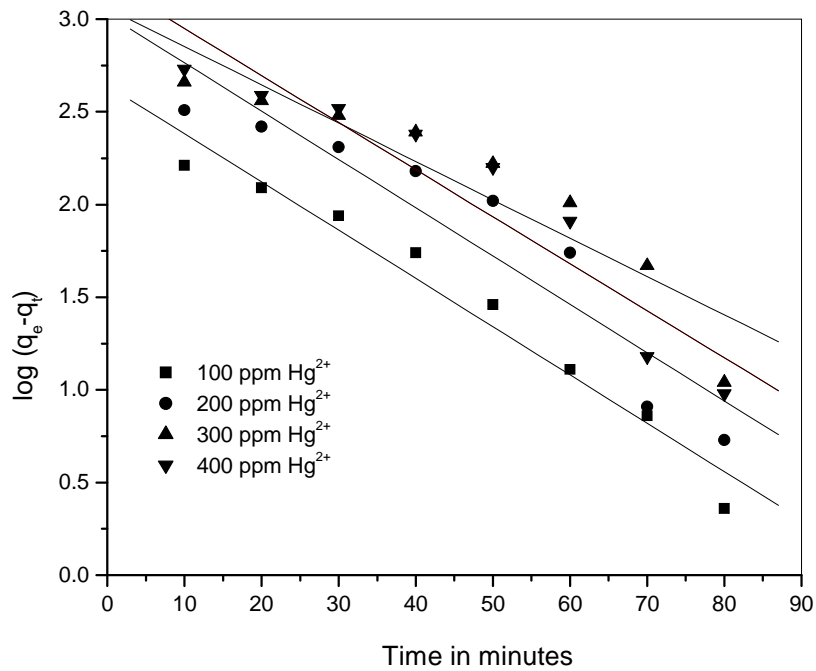


Fig. 9. Pseudo-first-order kinetic plot for the adsorption Hg(II) on ZNOs for different initial concentrations.

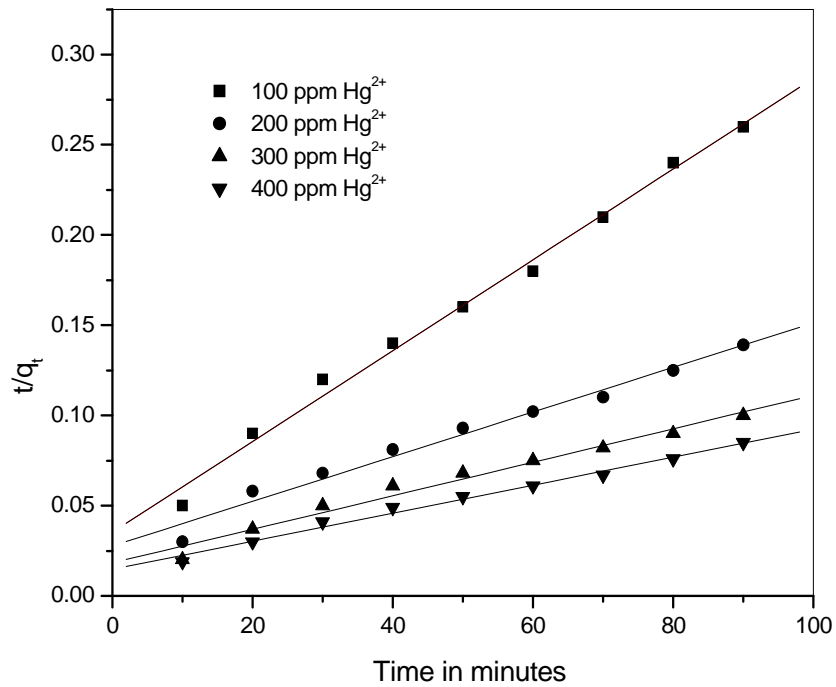


Fig. 10. Pseudo-second-order kinetic plot for the adsorption Hg(II) on ZNOs for different initial concentrations.

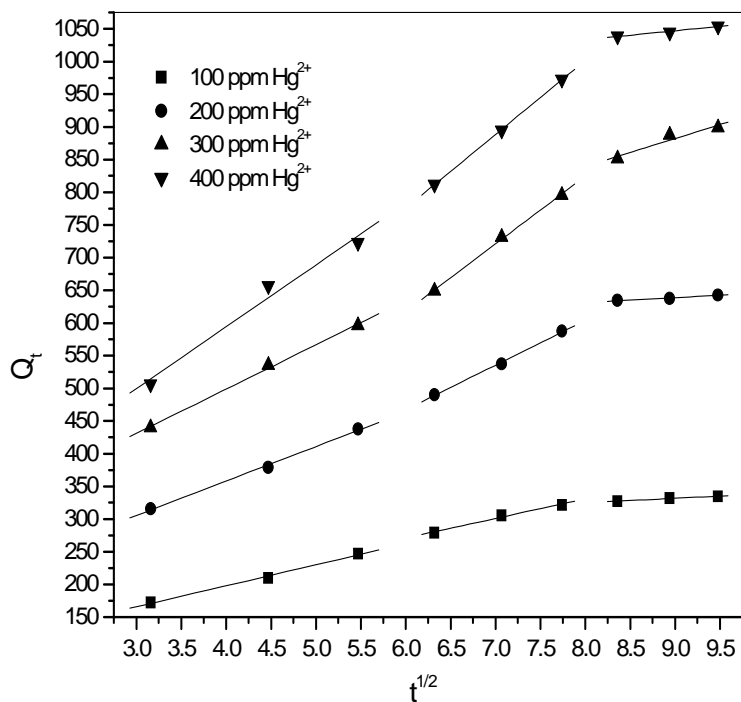


Fig. 11. Intraparticle diffusion kinetic model for adsorption Hg(II) on ZnOs.

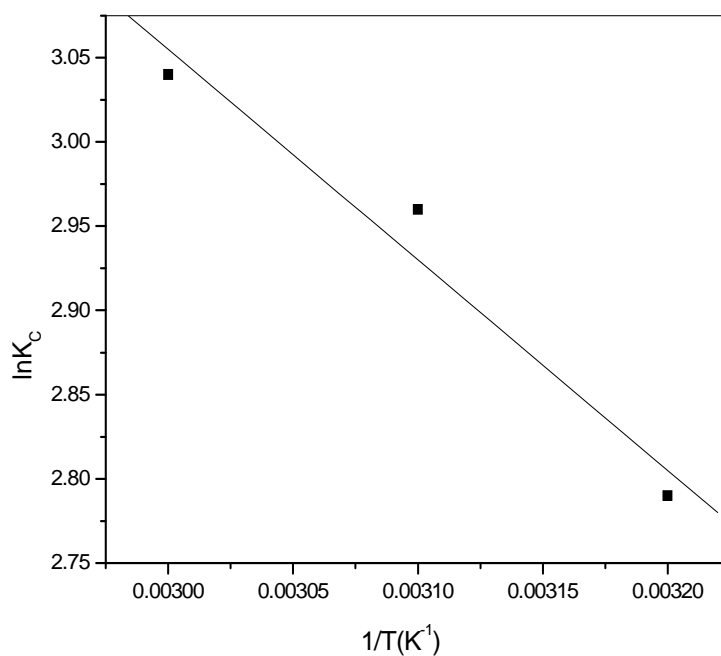


Fig. 12. Effect of temperature on adsorption of Hg(II) on ZnOs.

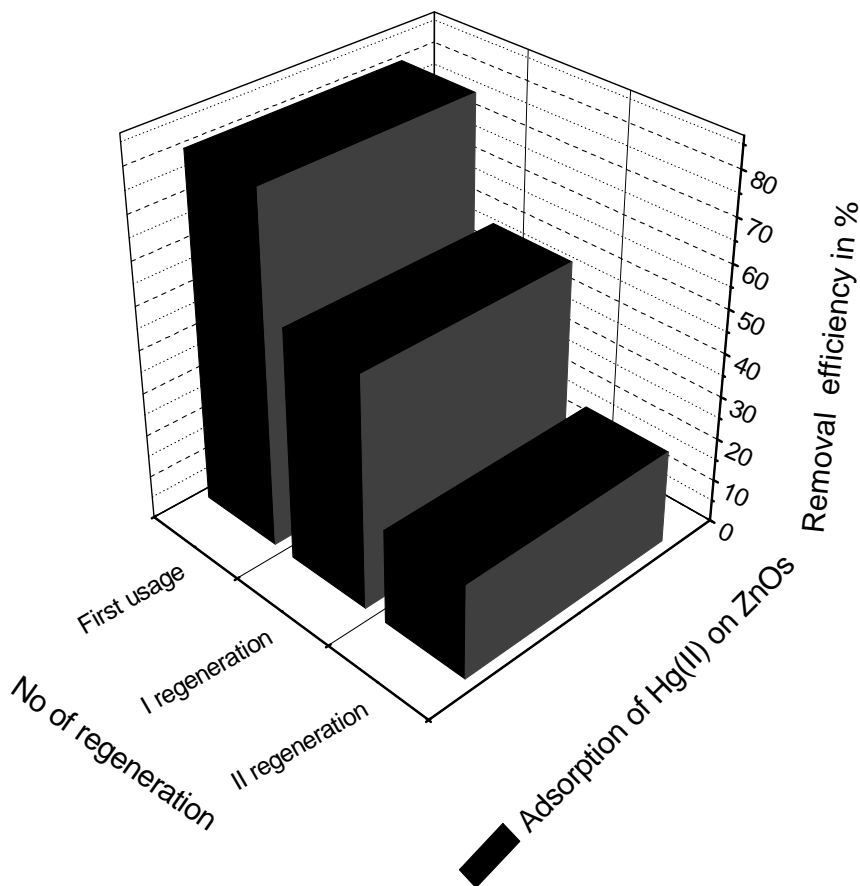


Fig. 13. Effect of ZNOs regeneration on removal efficiency of Hg(II) adsorption.

Table 1

Adsorbent	Phase	2θ	hkl	Size
ZNOs	ZnO	31.7	(100)	13.6
	ZnO	34.4	(002)	19.3
	ZnO	36.2	(101)	13.9
	NiO	43.2	(200)	11.1
	NiO	62.8	(220)	12.1

Parameters derived from XRD of ZNOs.

Table 2 Adsorption isotherm model parameters of adsorption of Hg(II) on ZNOs.

Metal ion	Langmuir			Freundlich		
	Q <sub>0</sub> (mg g <sup>-1</sup> )	K <sub>L</sub> (Lmg <sup>-1</sup> )	R <sup>2</sup>	K <sub>F</sub> (m <sup>n</sup> g <sup>-1</sup> )	n <sub>F</sub>	R <sup>2</sup>
Hg(II)	1474.9	0.01	0.99	107.1	2.2	0.90

**Table 3 Kinetic parameters for the adsorption of Hg (II) on ZNOs.**

Kinetic models	Parameters	Hg (II) concentration (mgL <sup>-1</sup> )			
		100	200	300	400
First order kinetics	q <sub>e,cal</sub> (m <sub>g</sub> g <sup>-1</sup> )	439	1058	1146	1592
	k <sub>1</sub> (min <sup>-1</sup> )	0.05	0.05	0.04	0.05
	R <sup>2</sup>	0.96	0.87	0.86	0.89
	q <sub>e,exp</sub> (m <sub>g</sub> g <sup>-1</sup> )	334	642	898	1054
Second order kinetics	q <sub>e,cal</sub> (m <sub>g</sub> g <sup>-1</sup> )	396	806	1077	1288
	k <sub>2</sub> (min <sup>-1</sup> )	0.07	0.04	0.05	0.05
	R <sup>2</sup>	0.99	0.97	0.97	0.98
	q <sub>e,exp</sub> (m <sub>g</sub> g <sup>-1</sup> )	334	642	898	1054

**Table 4 Thermodynamics parameters for the adsorption of Hg(II) on ZNOs.**

Temperature (°C)	Metal ion	ΔG <sup>0</sup> (kJmol <sup>-1</sup> )	ΔH <sup>0</sup> (kJmol <sup>-1</sup> )	ΔS <sup>0</sup> (JK <sup>-1</sup> mol <sup>-1</sup> )
30	Hg(II)	-7.03	-10.39	56.57
40		-7.70		
50		-8.16		

## CONCLUSION

ZNOs were prepared by homogeneous precipitation in aqueous solution with excess of sodium hydroxide and triton X-100 as capping agent. The pH of the solution played a significant role in the adsorption capacity of ZNOs powder. The maximum uptake was observed at the initial metal ion concentration (100 mgL<sup>-1</sup>). The R<sup>2</sup> values indicated that the adsorption of Hg(II) onto ZNOs gives better fit to Langmuir isotherm model when compare to Freundlich isotherm model. The adsorption capacities of ZNOs were found to be 1474.9 m<sub>g</sub>g<sup>-1</sup>. From the kinetic studies it was determined that the interactions could best explained on the basis of the second-order kinetic model. The thermodynamics studies revealed that the adsorption of Hg(II) on ZNOs is endothermic and spontaneous in nature. The above results confirmed the potential of ZNOs as an effective adsorbent for Hg(II) as well as other metal ions.

## Acknowledgements

The authors grateful to Visvesvaraya Technological University for providing financial support under research grant scheme (Project No VTU /Aca/2010-11/a-9/11353), The authors also grateful to K.S. Institute of Technology, Bangalore for providing the lab facility and to IIT Kanpur, IIT Bombay and PPRI Bangalore for providing instrumental facilities .

## REFERENCES

- [1] T Sheela; YA Nayaka; R Vishwanatha; S Basavanna; TG Venkatesha, *Powder Technol.*, **2012**, 217, 163–170.
- [2] SP Rodriguez; DF Calvino; JCN Munoz; MA Estevez; AN Delgadob; MJ Sanjurjo; EA Rodriguez, *J. Hazard. Mater.*, **2010**, 180,622–627.
- [3] SSM Hassan; NS Awwad; AHA Aboterika, *J. Hazard. Mater.*, **2008**, 154, 992–997.
- [4] VK Gupta; P Singh; N Rahman., *J. Colloid Interface Sci.*, **2004**, 275, 398–402.
- [5] M Visa; RA Carcel; L Andronic; A Duta, *Catal. Today.*, **2009**, 144, 137–142.
- [6] Y Liu; X Sun; B Li, *Carb. Poly.*, **2010**, 81, 335–339.
- [7] VK Gupta; PJM Carrott; MML Ribeiro; TL Suhas, *Crit. Rev. Env. Sci. Technol.*, **2009**, 39, 783-842.
- [8] D Sarkar; ME Essington; KC Misra, *Soil Sci. Soc. Am. J.*, **2000**, 641, 968–1975.
- [9] DG Kinniburgh; ML Jackson, *Soil Sci. Soc. Am. J.*, **1978**, 42, 45–47.
- [10] AI Adel; AE Ayman; A Ibrahim; M Hideyuki, *Adsorption.*, **2008**, 14, 21-29.
- [11] A Sharma; Pallavi; S Kumar, *Nano. Visi.*, **2011**, 3, 115-122.
- [12] B Pejova; T Kocareva; M Najdoski; I Grozdanov, *Appl. Surf. Sci.*, **2000**, 165, 271–278.
- [13] AA Kovalenko; AN Baranov; GN Panin, *Russ. J. Inorg. Chem.*, **2008**, 53, 1546–1551.
- [14] P Panneerselvam; N Morad; KA Tan, *J. Hazard. Mater.*, **2011**, 186(1), 160-168.
- [15] AA Ismail; A Ayman; E Midany; A Ibrahim; H Matsunaga, *Adsorption.*, **2008**, 14, 21–29.
- [16] LC Xiang; G Jie; P Jianming; Z Zulei; Y Yongsheng, *J. Environ. Sci.*, **2009**, 21, 1722–1729.
- [17] Z Temoçin; M Yigitoglu, *Water, Air, Soil Pollut.*, **2010**, 210, 463–472.
- [18] B Cheng; Y Le; W Cai; J Yu, *J. Hazard. Mater.*, **2011**, 185, 889–897.
- [19] MA Salam; RC Burk, *Wat. Air. Soil. Pollut.*, **2010**, 210, 101–111.

[20] J Sua; HG Huang; XY Jin; XQ Lu; ZL Chen, *J. Hazard. Mater.*, **2011**, 185, 63-70.